MiR-199a-5p-HIF-1α-STAT3 positive feed-back loop contributes to the progression of NSCLC

Xingping Yang
Sun Yat-sen University Sixth Affiliated Hospital
Yuzhen Zheng
Sun Yat-sen University Sixth Affiliated Hospital
Jian Tan
Affiliated Cancer Hospital and Institute of Guangzhou Medical University
Xiansheng Hu
Sun Yat-sen University Sixth Affiliated Hospital
Renjiang Tian
Affiliated Cancer Hospital and Institute of Guangzhou Medical University
Piao Shen
Affiliated Cancer Hospital and Institute of Guangzhou Medical University
Hongying Liao (sicuan923@163.com)
Sun Yat-sen University Sixth Affiliated Hospital https://orcid.org/0000-0002-7471-4415

Research

Keywords: miR-199a-5p, HIF-1α, STAT3, non-small cell lung cancer, Bevacizumab

Posted Date: August 12th, 2020

DOI: https://doi.org/10.21203/rs.3.rs-52959/v1

Abstract

Background

Non-small cell lung cancer (NSCLC), is the most common malignancy worldwide. MiR-199a-5p has been reported to play important roles in multiple tumors, inclusive of NSCLC. Whereas, little is definitively known pertaining to its explicit mechanism of action in NSCLC.

Methods

Expression of miR-199a-5p and HIF-1α mRNA were quantified employing qRT-PCR. H1299 and A549 cells were transiently transfected with miR-199a-5p mimics or inhibitors. Then CCK-8 assays, flow cytometry analysis, Transwell assay were implemented for detecting cell proliferation, cell cycle, apoptosis, migration and invasion of NSCLC cells, respectively. HIF-1α, STAT3 and p-STAT3 expression were detected via Western blotting. Bioinformatic analysis and dual-luciferase assay were performed for monitoring interaction between miR-199a-5p, HIF-1α and STAT3. Xenograft models were established with nude mice for further analyzing Bevacizumab resistance of NSCLC.

Results

MiR-199a-5p expression was markedly attenuated in NSCLC tissues and cell lines. Overexpression of miR-199a-5p constrained proliferation, migration, invasion but induced apoptosis of NSCLC cells. HIF-1α was identified as a direct target of miR-199a-5p. Further study confirmed a positive feed-back loop between miR-199a-5p, HIF-1α and STAT3. Co-transfection of HIF-1α or STAT3 overexpression plasmids counteracted effects of miR-199a-5p. Further study substantiated that feed-back loop might be in association with the Bevacizumab resistance of NSCLC cells .

Conclusion

MiR-199a-5p constrained the progression and Bevacizumab resistance of NSCLC by suppressing HIF-1α and STAT3, while HIF-1α/STAT3 axis suppressed the expression of miR-199a-5p, which forms a positive feed-back loop to promote the sustaining progression of NSCLC.

1 Introduction

Lung cancer, is the most common and leading cause of cancer-related death worldwide, among which, non-small cell lung cancer (NSCLC), accounts for more than 80% of cases [1]. Even though novel therapeutic approaches for NSCLC have significantly improved the the prognosis of the patients, almost all of the current approved drugs face the problem of drug resistance [2–4]. It's still necessary to further

clarify the mechanism of sustaining progression of NSCLC, which may provide clues for developing novel therapy strategies to improve the survival time of patients.

Non-coding RNAs, including microRNAs (miRNAs), participate in the pathogenesis of diverse human diseases, inclusive of NSCLC [5]. MiR-199a-5p, markedly downregulated in NSCLC tissues, is confirmed as a tumor suppressor: via directly targeting MAP3K11, miR-199a-5p suppresses proliferation and induces cell cycle arrest of A549 and H1299 cells [6]. Another research pointed out that overexpression of miR-199a-5p is capable of increasing doxorubicin sensitivity of A549 and H460 cells [7]. However, the explicit function and underlying mechanism whereby miR-199a-5p regulates NSCLC progression remain largely unknown.

Hypoxia inducible factor-1 (HIF-1α), defined as an oxygen-regulated protein, is in marked association with cancer biology [8]. Of note, in NSCLC, HIF-1α was substantiated to be an oncogene. For example, subsequent to knockdown of HIF-1α with siRNA, proliferation and invasion of NCI-H157 cells were constrained but apoptosis was promoted [9]. Signal transducer and activator of transcription 3(STAT3) is also identified as a promoter for NSCLC. For instance, downregulation of STAT3 weakens colony forming ability and proliferation of A549 and SK-MES-1 cells [10]. Nonetheless, the mechanism of HIF-1α and STAT3 hyperactivation in NSCLC has not been clarified clearly.

Intriguingly, HIF-1α, reportedly, is noted to activate STAT3 by repressing miR-34a [11]. It is noteworthy that, STAT3 knockdown in cardiomyocyte of neonatal rat enhanced the miR-199a-5p promoter activity, and miR-199a-5p expression is demonstrably augmented, suggesting that STAT3 negatively regulates miR-199a-5p [12]. Besides, bioinformatic analysis implicated that potential binding sites existed between miR-199a-5p and HIF-1α. Based on these information, we supposed that miR-199a-5p-HIF-1α-STAT3 could probably be a positive feed-back loop in NSCLC development (Fig. 1). This study was designed to validate this scientific hypothesis.

2 Materials And Methods

2.1 Clinical samples

30 patients with NSCLC in the absence of radiotherapy or chemotherapy prior to surgery in our hospital from 2017 to 2018 were enrolled in this research. 30 pairs of NSCLC tissues/ corresponding adjacent lung tissues as well as blood samples of all subjects were obtained during the surgery. All tissue samples were immediately cryopreserved in liquid nitrogen at − 196 °C posterior to the resection. The study was approved by the Ethics Committees of the Sixth Affiliated Hospital of Sun Yat-sen University. Written informed consents were acquired from every participating patient. The procedures were performed under the instruction of the principles of the Declaration of Helsinki.

2.2 Cell culture and transfection

NSCLC cell lines (H1299, H157, A549 and H460) and normal human lung epithelial cells BEAS-2B were obtained from American Type Culture Collection (ATCC, Rockville, MD, USA) or China Center for Type Culture Collection (Wuhan, China), and cultivated in RPMI-1640 medium (Gibco, Carlsbad, CA, USA) supplemented with 10% fetal bovine serum (FBS) (Gibco, Carlsbad, CA, USA) at 37 °C with 5% CO_2. For experimentally analyzing the resistance of NSCLC cells to Bevacizumab, A549 cells were treated with 10 μM Bevacizumab (Topscience, Shanghai, China).

Construction of miR-199a-5p mimics, control of mimics, miR-199a-5p inhibitors, control of inhibitors, overexpression plasmids of HIF1A, STAT3 and their negative control (vector) was accomplished by Genepharma (Shanghai, China). By the time of reaching 60% confluence, A549 and H1299 cells were transiently transfected with miR-199a-5p inhibitors, miR-199a-5p mimics or the overexpression plasmids employing Lipofectamine^{TM}3000 (Invitrogen, Carlsbad, CA, USA) in conformity with manufacture's protocols. Transfection efficiency was validated 24 h after the transfection with quantitative real-time polymerase chain reaction (qRT-PCR).

2.3 qRT-PCR

Isolation of total RNA from NSCLC tissues, blood samples and cells was accomplished utilizing TRIzol reagent (Invitrogen, Carlsbad, CA, USA). Reverse transcription of total RNA to cDNA was performed with reverse transcription kit (TaKaRa, Dalian, China). With the cDNA as template, qRT-PCR was performed utilizing SYBR Premix Ex Taq ™ II (Takara, Shiga, Japan) on ABI 7500 Fast Real-Time PCR System (Applied Biosystems, Waltham, MA, UK). The primer sequences utilized in our current research were illustrated in supplementary Table 1.

2.4 Cell counting kit-8 (CCK-8) assay

A549 and H1299 cells were seeded into 96-well plates (2×10^3 per well). Followed by culture for 24, 48, 72 and 96 h, each well was supplemented with 10 μL CCK-8 solution (Dojindo, Tokyo, Japan). After CCK-8 solution was added, and the cells were incubated for 1 h. Then cell viability at each time point was evaluated by measuring the absorbance values at a wavelength of 450 nm. Then the proliferation curve was plotted.

2.5 Flow cytometery analysis

For cell cycle analysis,A549 or H1299 cells were seeded into 6-well plate (5×10^5 cells / well) and cultured in 0.2% serum medium for 24 h for synchronization. Subsequently, the cells were stained with propidium iodide (PI) solution (Beyotime, Shanghai, China) and were examined employing a FACS flow cytometer (BD Biosciences, San Jose, CA, USA). For apoptosis analysis A549 and H1299 cells were collected, washed, fixed, and permeabilized. Then Annexin V-FTIC/PI Apoptosis Detection Kit (KeyGen, Nanjing, China) was employed to detect the apoptosis of the cells according to the manufacturer's instruction. The data were computationally analyzed deploying ModFit software (BD Biosciences, San Jose, CA, USA) (for cell cycle analysis) or Flowjo V10 software (BD Biosciences, San Jose, CA, USA) (for apoptosis analysis).

2.6 Transwell assay

The pore size of the aperture in the membrane of Transwell chambers (Corning, Shanghai, China) was 8 μm. The chambers were coated with Matrigel (Sigma, Shanghai, China) for determination of invasive ability. No matrigel was added in the migration assay. The lower compartment of the Transwell system was filled with 600 μL RPMI-1640 medium containing 10% FBS, and the upper compartment contained 200 μL cell suspension (5×10^5 cells in each well in serum-free medium). The cells were cultivated for 48 h, and then the Transwell chambers were taken out. The cells that failed to migrate were removed with cotton swabs. Then the remaining cells attached on the lower surface of the Transwell membrane were fixed with 4% paraformaldehyde for 20 min, and stained with 0.5% crystal violet solution. Ultimately, 5 random fields of each Transwell membrane were randomly selected and the numbers of stained cells were reckoned under a microscope.

2.7 Dual-luciferase reporter assay

The fragment of wild type (WT) or mutant (MUT) HIF1A 3' UTR was inserted into a pmirGLO -dual-luciferase miRNA target expression vector (Promega, Madison, WI, USA). The recombinant reporter vectors were co-transfected into H1299 cells with miR-199a-5p mimics or mimics control and then the cells were cultivated for 48 h. Luciferase activity was subsequently measured utilizing Dual Luciferase Reporter Gene Assay Kit (Beyotime, Jiangsu, China) in conformity with manufacturer's protocol. The luciferase activity of firefly was normalized to that of of renilla.

2.8 Western blotting

NSCLC cells in each group were harvested and washed three times with cold PBS, and 100 μL RIPA lysate (Beyotime, Shanghai, China) was added. The cells were lysed in ice-bath for 30 min to extract the total protein. The mixtures were succeedingly centrifuged at 12,000 rpm for 20 min, and the supernatant was collected as the protein samples. The protein samples were denatured, separated by sodium dodecylsulfate-polyacrylamide gel-electrophoresis, and transferred onto PVDF membranes (Millipore, Bedford, MA, USA). The membranes were then blocked with 5% skimmed milk, and incubated with primary antibodies [Rabbit Anti-STAT3 (phospho S727) antibody, 1:1000, ab32143; Rabbit Anti-STAT3 antibody, 1:1000, ab68153; Rabbit Anti-HIF-1 alpha antibody, 1:1000, ab82832] at 4 °C overnight. Afterward, the membranes were washed with TBST buffer and then incubated with secondary horseradish peroxidase (HRP-) labeled goat anti-rabbit IgG antibodies (1:2000, ab205718, Abcam, Shanghai, China) for additional 2 h at room temperature. β-actin was employed as internal reference. The protein bands on the membranes were then detected utilizing ECL kit (Amersham Pharmacia Biotech, Little Chalfont, UK) and computationally analyzed by deploying Image J software (National Institutes of Health, Bethesda, MD, USA).

2.9 Xenografts models

The procedures of animal experiments have been reviewed and approved by the Animal Ethics Committee of the Sixth Affiliated Hospital of Sun Yat-sen University and in compliance with the National Institute of Health Guidelines for Care and Use of Laboratory Animals in Biomedical Research. A549 cells, previously reported to be resistant to Bevacizumab, were selected for establishing xenografts models.

Subsequent to transfection with miR-199a-5p mimics, miR-199a-5p inhibitors, HIF-1α and STAT3 overexpression plasmid or their negative controls, A549 cells were inoculated subcutaneously into the right flank region of male athymic (BALB/c-nu) mice (6 weeks old). By the time of tumor size reached approximately 100 mm^3, 27 mice were randomly divided into nine groups with 3 mice per group: Blank group (no treatment), BV group (mice were injected with 10 mg/kg Bevacizumab weekly), BV + control of mimics group (A549 cells were transfected with control of mimics prior to injection and mice were injected with 10 mg/kg Bevacizumab weekly. As for the rest groups, A549 cells were transiently transfected with different plasmids or oligonucleotides prior to injection and mice were injected with 10 mg/kg Bevacizumab weekly: BV + control of inhibitors group, BV + miR-199a-5p mimics group, BV + miR-199a-5p inhibitors group, BV + miR-199a-5p mimics + vector group, BV + miR-199a-5p mimics + HIF-1α group, BV + miR-199a-5p mimics + STAT3 group. The tumor volume was recorded every two days. The tumor volume (in mm^3) was calculated with the formula 0.5 × L × W2 (L = length, W = width).

2.10 Statistical analysis

All statistical analyses were carried out utilizing SPSS 23.0 software (SPSS Inc., Chicago, IL, USA). Data were presented as the means ± SE. Data were examined whether they were normally distributed with the One Sample Kolmogorov-Smirnov test. As for the data normally distributed, t-test or one-way ANOVA test was performed. As for the data not normally distributed, rank test was conducted. $P < 0.05$ was deemed to be statistically significant.

3 Results

3.1 Expression of miR-199a-5p was down-regulated in NSCLC

GSE135918 contained the miRNA expression profile of 5 fresh lung cancer tissues and 5 fresh non-tumor lung tissues. It was reanalyzed, and it was noted that miR-199a-5p was dramatically downregulated in NSCLC tissues versus normal lung tissues (Fig. 2A, B). Consistently, qRT-PCR data manifested that miR-199a-5p was notably reduced in NSCLC tissues as opposed to adjacent normal lung tissues (Fig. 3A). Additionally, miR-199a-5p was observed to be reduced in serum samples of NSCLC patients versus healthy subjects (Fig. 3B). The downregulation of miR-199a-5p in NSCLC was further validated in GSE53882 and ENCORI database (Fig. 3C, D). Furthermore, miR-199a-5p expression was demonstrated to be underexpressed in NSCLC cell lines compared with normal lung epithelial cells BASE-2B (Fig. 3E).

3.2 MiR-199a-5p repressed proliferation, migration and invasion of NSCLC

MiR-199a-5p mimics and miR-199a-5p inhibitors were transfected into H1299 and A549 cells, based upon that miR-199a-5p expression was lowest in H1299 cells and highest in A549 cells (Fig. 4A). Through CCK-8 assay, miR-199a-5p was noted to prominently dampen the proliferation of H1299 cells, while the

reversed effect was observed in A549 cells with miR-199a-5p inhibited (Fig. 4B, C). Furthermore, flow cytometry analysis implicated that H1299 cells were arrested in G0/G1 phase after miR-199a-5p was overexpressed whereas miR-199a-5p inhibitors induced more A549 cells entering S phase (Fig. 4D). What's more, the apoptosis of H1299 and A549 cells was analyzed and it was noted that miR-199a-5p overexpression promoted the apoptosis of NSCLC cells (Fig. 4E). Additionally, Transwell assays suggested that miR-199a-5p constrained the migration and invasion of NSCLC cells, while inhibiting miR-199a-5p promoted the migration and invasion of NSCLC cells (Fig. 4F, G). Collectively, these data validated that miR-199a-5p was tumor suppressor of NSCLC.

3.3 HIF-1α was confirmed as a target gene of miR-199a-5p

miRmap, miRanda and TargetScan database were searched for the downstream target genes of miR-199a-5p and 221 genes were predicted by all of the three database (Fig. 5A). HIF1A, the gene of HIF-1α, previously reported to exert a tumor promoting role in NSCLC [9, 13], was among them (Fig. 5B). Dual-luciferase reporter assay was employed for verifying the binding site, and as shown, miR-199a-5p mimics remarkably suppressed luciferase activity of wild type HIF1A reporter, whereas this effect was abolished when the binding site was mutated (Fig. 5C). Furthermore, via qRT-PCR and Western blotting, it was demonstrated miR-199a-5p is capable of repressing the expressions of HIF-1α mRNA and protein, while inhibiting miR-199a-5p promoted the expression of HIF-1α in NSCLC cells (Fig. 5D, E). Besides, HIF-1α expression in NSCLC cell lines and tissues was significantly up-regulated (Fig. 5F, G). Moreover, the expression of miR-199a-5p in NSCLC tissues was in negative correlation with HIF1A (Fig. 5H). These data confirmed the targeting relationship between miR-199a-5p and HIF1A.

3.4 The positive feed-back loop among miR-199a-5p, HIF1α and STAT3

Subsequently, expression of STAT3 mRNA was measured by qRT-PCR, the results of which displayed that STAT3 was up-regulated in NSCLC tissues, in negative correlation with miR-199a-5p whereas in positive correlation with HIF-1α (Fig. 6A-C). Followed by miR-199a-5p overexpression or inhibition in NSCLC cells, no obvious alteration was noted in STAT3 expression, whereas miR-199a-5p was observed to inactivate STAT3 phosphorylation. Besides, it was demonstrated that HIF-1α overexpression activated phosphorylation of STAT3, while STAT3 overexpression further reduced miR-199a-5p expression (Fig. 6D-J). Collectively, these data a positive feed-back loop of miR-199a-5p-HIF-1α-STAT3 exists in NSCLC.

3.5 HIF-1α and STAT3 counteracted effects of miR-199a-5p on NSCLC

MiR-199a-5p mimics and HIF-1α or STAT3 overexpression plasmids were transiently co-transfected into H1299 cells so as to further authenticate interaction between miR-199a-5p, HIF-1α and STAT3. As expected, effects of miR-199a-5p on proliferation, cell cycle, apoptosis, migration and invasion were

reversed by HIF-1α overexpression or STAT3 overexpression (Fig. 7A-F), which supported that miR-199a-5p regulated the malignancy of NSCLC cells by means of modulating HIF-1α and STAT3.

3.6 MiR-199a-5p enhanced sensitivity of A549 cells to Bevacizumab

High expression of HIF-1α and the activation of STAT3 signaling are reported to be conducive to resistance to Bevacizumab [14, 15]. Therefore, we supposed that miR-199a-5p could be a potential therapeutic target for sensitizing NSCLC cells to Bevacizumab treatment. A549 cells, previously reported to show moderate resistance to Bevacizumab treatment [16], were used for subsequent experiments. MiR-199a-5p mimics or inhibitors were transiently transfected into A549 cells, and then the cells were treated with Bevacizumab (10 μM). Next, the expressions of HIF-1α, STAT3 and p-STAT3 were measured utilizing qRT-PCR, the results of which suggested that miR-199a-5p inhibited the expression of HIF-1α and activation of STAT3 (Fig. 8A-E). Through CCK-8 assay and flow cytometry, miR-199a-5p mimics were demonstrated to remarkably inhibit the viability and promote the apoptosis induced by Bevacizumab; conversely, miR-199a-5p inhibitors repressed the viability of A549 cells, and promoted the apoptosis induced by Bevacizumab (Fig. 8F-H). Consistently, the results of *in vivo* experiments suggested that miR-199a-5p facilitated the tumor-suppressive effects of Bevacizumab, while miR-199a-5p counteracted the tumor cytotoxicity of Bevacizumab (Fig. 8I, J). Collectively, these findings indicated that miR-199a-5p enhanced sensitivity of A549 cells to Bevacizumab.

3.7 HIF-1α and STAT3 enhanced resistance of A549 cells to Bevacizumab

For further deciphering whether miR-199a-5p increased the sensitivity of A549 cells to Bevacizumab by suppressing the expression of HIF-1α and the activation of STAT3, miR-199a-5p mimics and HIF-1α or STAT3 overexpression plasmids were co-transfected into A549 cells (Fig. 9A-E). It was experimentally implicated that both HIF-1α and STAT3 were capable of remarkably eliminating the effects of miR-199a-5p on the sensitivity of A549 cells to Bevacizumab *in vitro* and *in vivo* (Fig. 9F-J). These data validated that miR-199a-5p was capable of sensitizing A549 cells to Bevacizumab through regulating HIF-1α and STAT3.

4 Discussion

Multiple miRNAs have been identified as potential diagnostic biomarkers and therapeutic targets for NSCLC. For example, expression of miR-128-3p was significantly up-regulated in NSCLC tissues by comparison with adjacent normal tissues; its overexpression remarkably induced the migration and invasion of A549, Calu-3 and H520 cells [17]. In the present research, miR-199a-5p was found to be dramatically down-regulated in NSCLC tissues, serum samples of NSCLC patients and multiple NSCLC cell lines. Gain-of-function and loss-of-function experiments further illustrated that miR-199a-5p

constrained the proliferation, migration and invasion, and facilitated the apoptosis of NSCLC cells, indicative of a prospective value regarding miR-199a-5p in NSCLC therapeutics. Some other studies also demonstrate that miR-199a-5p represses the malignancy of NSCLC cell lines, such as H1299, A549 and SPCA-1 cells, which is consistent with our demonstrations [18, 19]. The underexpression of miR-199a-5p in NSCLC has been reported by several previous reports [6, 7, 18, 19]. “competitive endogenous RNA (ceRNA)” mechanism can probably contribute to the dysregulation of miR-199a-5p in NSCLC. It is reported that, LINC01123 sponges miR-199a-5p as a ceRNA to negatively regulate its expression in NSCLC cells [18]; similarly, in NSCLC cells, miR-199a-5p is reported to be adsorbed and repressed by lncRNA PVT1 [19]. Interestingly, in cardiomyocytes, pSTAT3 is able to bind to the promoter region of miR-199a-2 gene, and can repress its transcription and down-regulate its expression, which is more significant under hypoxic conditions, suggesting miR-199a-5p is modulated by STAT3 signaling and HIF-1α signaling [12, 20]. In the present study, for the first time, we demonstrated that overexpression of STAT3 or HIF-1α increased the expression of miR-199a-5p in NSCLC cells, which indicated that the hypoxic tumor microenvrionment and activation of STAT3 signaling contributed the dysregulation of miR-199a-5p in NSCLC cells.

HIF-1α, recognized as oxygen-labile subunit of HIF-1, contains the transactivation domains responsible for HIF-1α transcriptional activity [21, 22]. Despite the fact that HIF-1α is merely highly expressed during hypoxic condition, it is also detectable in normoxic condition. Hypoxia is a common characteristic in the microenvironment of various types of solid tumors, promoting HIF-1α expression [22–24]. In turn, HIF-1α is conducive to the adjustment of tumors to hypoxia through transcriptional activation of more than 100 downstream genes including LEP, EPO, PKM, etc; in this regard, HIF-1α further promotes proliferation and growth of tumor cells [23]. In NSCLC, HIF-1α is up-regulated in tumor tissues and cell lines, and its overexpression facilitates the proliferation, migration and invasion of cancer cells; what’s more, the 5-year survival rate of patients with low expression level of HIF-1α is higher than those with high expression level of HIF-1α [25–27]. For shedding more light upon the underlying mechanism by which miR-199a-5p exhibited its tumor-suppressive role in NSCLC, miRmap, miRanda and TargetScan databases were employed for prediction of target gene of miR-199a-5p in this study. Interestingly, the gene of HIF-1α, HIF1A, was validated as a target gene of miR-199a-5p in NSCLC in the present study. Our data suggested that the dysregulation of HIF-1α in NSCLC is not only due to the hypoxic microenvrionment, but also partly resulted from the down-regulation of upstream miRNAs.

STAT3, a member of signal transducer and activator of transcription (STAT) family, regulates the expressions of genes relevant to cell cycle, cell survival, and immune response. In recent years, STAT3 has been found to be constitutively activated in multiple types of human cancers, indicating that STAT3 is a valuable target for cancer therapy [28]. STAT3 has been identified to be abnormally increased in NSCLC tissues and cell lines, and knockdown of STAT3 can induce apoptosis, reduce proliferation, migration and invasion of A549 and H1975 cells [29]. Consistently, we demonstrated that transfection of STAT3 overexpression plasmids notably induced proliferation, migration and invasion of NSCLC cells. It is noteworthy that HIF-1α is previously reported to activate STAT3 by means of repressing miR-34a in colorectal cancer [11]. Furthermore, in head and neck squamous cell carcinoma, with static inhibition of

STAT3 activation, expression in HIF-1α was repressed [30]. In the present work, we demonstrated that HIF-1α overexpression activated STAT3, and STAT3 overexpression repressed the expression of miR-199a-5p, but promoted the expression of HIF-1α. Altogether, our study presented a novel positive feed-back loop, which was formed by miR-199a-5p, HIF-1α and STAT3 in NSCLC, and this positive feed-back loop is crucial to clarify the mechanism of hyperactivation of HIF-1α pathway and STAT3 signaling in NSCLC tissues.

At the last part of our present study, we analyzed the sensitivity of A549 cells to Bevacizumab and found the positive feed-back loop also contributed to Bevacizumab sensitivity. Bevacizumab, possessing high efficacy and safety, is a monoclonal anti-VEGF antibody and an encouraging target drug for NSCLC, particularly advanced NSCLC patients [31, 32]. There remains little study investigating the molecular mechanism regarding Bevacizumab sensitivity in NSCLC at the present. We found the positive feed-back loop miR-199a-5p-HIF-1α-STAT3 also exists after Bevacizumab treatment and miR-199a-5p enhanced sensitivity of A549 cells to Bevacizumab. Our study provides a new thought to further improve outcomes for Bevacizumab therapy. miR-199a-5p may have the potential to improve prognosis for NSCLC patients in advanced stages.

5 Conclusion

In aggregate, our research confirmed a positive feed-back loop among miR-199a-5p, HIF-1α and STAT3. The loop contributes to NSCLC progression and resistance to Bevacizumab. The results provide important information regarding molecular regulating networks in NSCLC.

Declarations

Ethics approval and consent to participate

Our research was approved by the Sixth Affiliated Hospital of Sun Yat-sen University. Written informed consents were acquired from each participant and all protocols were conducted in accordance with the principles of the Declaration of Helsinki. For animal experiments, all procedures were reviewed and approved by the Animal Study Committee of the Sixth Affiliated Hospital of Sun Yat-sen University and were performed in compliance with the National Institutes of Health Guide for the Care and Use of Laboratory Animals and Animal Welfare Act.

Consent for publication

Not applicable.

Availability of data and material

The data used to support the findings of this study are available from the corresponding author upon request.

Competing interests

The authors declare that they have no competing interests.

Funding

Not applicable.

Authors' contributions

Conceived and designed the experiments: HYL; Performed the experiments: XPY, YZZ and JT; Statistical analysis: XPY, JT and RJT; Wrote the paper: XPY, XSH, RJT and PS.

Acknowledgements

Not applicable.

References

1. Bradbury P, Sivajohanathan D, Chan A, Kulkarni S, Ung Y, Ellis PM. Postoperative Adjuvant Systemic Therapy in Completely Resected Non-Small-Cell Lung Cancer: A Systematic Review. Clin Lung Cancer. 2017 May;18(3):259–73.e8.
2. Yu X, Ding Q, Hu C, Mu G, Deng Y, Luo Y, Yuan Z, Yu H, Liu L. Evaluating micro-optical coherence tomography (μOCT) as a feasible imaging tool for pancreatic disease diagnosis. IEEE JSTQE. 2018 April 16; 1–1.
3. Brody R, Zhang Y, Ballas M, Siddiqui MK, Gupta P, Barker C, Midha A, Walker J. PD-L1 expression in advanced NSCLC: Insights into risk stratification and treatment selection from a systematic literature review. Lung Cancer. 2017 Oct;112:200–15.
4. Zheng H, Zhan Y, Liu S, Lu J, Luo J, Feng J, Fan S. The roles of tumor-derived exosomes in non-small cell lung cancer and their clinical implications. J Exp Clin Cancer Res. 2018 Sep 14;37(1):226.
5. Tu Z, He D, Deng X, Xiong M, Huang X, Li X, Hao L, Ding Q, Zhang Q. An eight-long non-coding RNA signature as a candidate prognostic biomarker for lung cancer. Oncol Rep. 2016 Jul;36(1):215–22.
6. Li Y, Wang D, Li X, Shao Y, He Y, Yu H, Ma Z. MiR-199a-5p suppresses non-small cell lung cancer via targeting MAP3K11. J Cancer. 2019 Jun 2;10(11):2472–2479.
7. Jin Y, Wang H, Zhu Y, Feng H, Wang G, Wang S. miR-199a-5p is involved in doxorubicin resistance of non-small cell lung cancer (NSCLC) cells. Eur J Pharmacol. 2020 Jul;5:878:173105.
8. Semenza GL. Targeting HIF-1 for cancer therapy. Nat Rev Cancer. 2003 Oct;3(10):721–32.
9. Qian J, Bai H, Gao Z, Dong YU, Pei J, Ma M, Han B. Downregulation of HIF-1α inhibits the proliferation and invasion of non-small cell lung cancer NCI-H157 cells. Oncol Lett. 2016 Mar;11(3):1738–44.
10. Yin ZJ, Jin FG, Liu TG, Fu EQ, Xie YH, Sun RL. Overexpression of STAT3 potentiates growth, survival, and radioresistance of non-small-cell lung cancer (NSCLC) cells. J Surg Res. 2011 Dec;171(2):675–

83.

11. Li H, Rokavec M, Jiang L, Horst D, Hermeking H. Antagonistic Effects of p53 and HIF1A on microRNA-34a Regulation of PPP1R11 and STAT3 and Hypoxia-induced Epithelial to Mesenchymal Transition in Colorectal Cancer Cells. Gastroenterology. 2017 Aug;153(2):505–20.
12. Haghikia A, Missol-Kolka E, Tsikas D, Venturini L, Brundiers S, Castoldi M, Muckenthaler MU, Eder M, Stapel B, Thum T, Haghikia A, Petrasch-Parwez E, Drexler H, Hilfiker-Kleiner D, Scherr M. Signal transducer and activator of transcription 3-mediated regulation of miR-199a-5p links cardiomyocyte and endothelial cell function in the heart: a key role for ubiquitin-conjugating enzymes. Eur Heart J. 2011 May;32(10):1287–97.
13. Lin CW, Wang LK, Wang SP, Chang YL, Wu YY, Chen HY, Hsiao TH, Lai WY, Lu HH, Chang YH, Yang SC, Lin MW, Chen CY, Hong TM, Yang PC. Daxx inhibits hypoxia-induced lung cancer cell metastasis by suppressing the HIF-1α/HDAC1/Slug axis. Nat Commun. 2016;7:13867.
14. Jahangiri A, De Lay M, Miller LM, Carbonell WS, Hu YL, Lu K, Tom MW, Paquette J, Tokuyasu TA, Tsao S, Marshall R, Perry A, Bjorgan KM, Chaumeil MM, Ronen SM, Bergers G, Aghi MK. Gene Expression Profile Identifies Tyrosine Kinase c-Met as a Targetable Mediator of Antiangiogenic Therapy Resistance. Clin Cancer Res. 2013 Apr 1;19(7):1773-83.
15. Hartwich J, Orr WS, Ng CY, Spence Y, Morton C, Davidoff AM. HIF-1α Activation Mediates Resistance to Anti-Angiogenic Therapy in Neuroblastoma Xenografts. J Pediatr Surg. 2013 Jan;48(1):39–46.
16. Wang Y, Yan P, Liu Z, Yang X, Wang Y, Shen Z, Bai H, Wang J, Wang Z. MEK inhibitor can reverse the resistance to bevacizumab in A549 cells harboring Kirsten rat sarcoma oncogene homolog mutation. Thorac Cancer. 2016 Apr 26;7(3):279–87.
17. Weidle UH, Birzele F, Nopora A. MicroRNAs as Potential Targets for Therapeutic Intervention With Metastasis of Non-small Cell Lung Cancer. Cancer Genomics Proteomics. 2019;16(2):99–119.
18. Hua Q, Jin M, Mi B, Xu F, Li T, Zhao L, Liu J, Huang G. LINC01123, a c-Myc-activated long non-coding RNA, promotes proliferation and aerobic glycolysis of non-small cell lung cancer through miR-199a-5p/c-Myc axis. J Hematol Oncol. 2019 Sep 5;12(1):91.
19. Wang C, Han C, Zhang Y, Liu F. LncRNA PVT1 regulate expression of HIF1α via functioning as ceRNA for miR–199a–5p in non–small cell lung cancer under hypoxia. Mol Med Rep. 2018 Jan;17(1):1105–10.
20. Zhou Y, Pang B, Xiao Y, Zhou S, He B, Zhang F, Liu W, Peng H, Li P. The protective microRNA-199a-5p-mediated unfolded protein response in hypoxic cardiomyocytes is regulated by STAT3 pathway. J Physiol Biochem. 2019 Feb;75(1):73–81.
21. Tirpe AA, Gulei D, Ciortea SM, Crivii C, Berindan-Neagoe I. Hypoxia. Overview on Hypoxia-Mediated Mechanisms with a Focus on the Role of HIF Genes. Int J Mol Sci. 2019 Dec 5;20(24):6140.
22. Albadari N, Deng S, Li W. The Transcriptional Factors HIF-1 and HIF-2 and Their Novel Inhibitors in Cancer Therapy Expert Opin Drug Discov. 2019 Jul;14(7):667–682.
23. Masoud GN, Li W. HIF-1α Pathway: Role, Regulation and Intervention for Cancer Therapy Acta Pharm Sin B. 2015 Sep;5(5):378–89.

24. Gu Q, He Y, Ji J, Yao Y, Shen W, Luo J, Zhu W, Cao H, Geng Y, Xu J, Zhang S, Cao J, Ding WQ. Hypoxia-inducible Factor 1α (HIF-1α) and Reactive Oxygen Species (ROS) Mediates Radiation-Induced Invasiveness Through the SDF-1α/CXCR4 Pathway in Non-Small Cell Lung Carcinoma Cells Oncotarget. 2015 May 10;6(13):10893-907.
25. He J, Hu Y, Hu M, Zhang S, Li B. The relationship between the preoperative plasma level of HIF-1α and clinic pathological features, prognosis in non-small cell lung cancer. Sci Rep. 2016 Feb 8;6:20586.
26. Jing XG, Chen TF, Huang C, Wang H, An L, Cheng Z, Zhang GJ. MiR-15a Expression Analysis in Non-Small Cell Lung Cancer A549 Cells Under Local Hypoxia Microenvironment Eur Rev Med Pharmacol Sci. 2017 May;21(9):2069–2074.
27. Chi Y, Luo Q, Song Y, Yang F, Wang Y, Jin M, Zhang D. Circular. RNA circPIP5K1A Promotes Non-Small Cell Lung Cancer Proliferation and Metastasis Through miR-600/HIF-1α. Regulation J Cell Biochem. 2019 Nov;120(11):19019–30.
28. Furtek SL, Backos DS, Matheson CJ, Reigan P. Strategies and Approaches of Targeting STAT3 for Cancer Treatment ACS Chem Biol. 2016 Feb 19;11(2):308–18.
29. Li ZY, Zhang ZZ, Bi H, Zhang QD, Zhang SJ, Zhou L, Zhu XQ, Zhou J. MicroRNA–4500 Suppresses Tumor Progression in Non–small Cell Lung Cancer by Regulating STAT3 Mol Med Rep. 2019 Dec;20(6):4973–4983.
30. Adachi M, Cui C, Dodge CT, Bhayani MK, Lai SY. Targeting STAT3 inhibits growth and enhances radiosensitivity in head and neck squamous cell carcinoma. Oral Oncol. 2012 Dec;48(12):1220–6.
31. Besse B, Le Moulec S, Mazières J, Senellart H, Barlesi F, Chouaid C, Dansin E, Bérard H, Falchero L, Gervais R, Robinet G, Ruppert AM, Schott R, Léna H, Clément-Duchêne C, Quantin X, Souquet PJ, Trédaniel J, Moro-Sibilot D, Pérol M, Madroszyk AC, Soria JC. Bevacizumab in Patients With Nonsquamous Non-Small Cell Lung Cancer and Asymptomatic, Untreated Brain Metastases (BRAIN): A Nonrandomized, Phase II Study. Clin Cancer Res. 2015 Apr 15;21(8):1896 – 903.
32. Assoun S, Brosseau S, Steinmetz C, Gounant V, Zalcman G. Bevacizumab in Advanced Lung Cancer: State of the Art Future Oncol. 2017 Dec;13(28):2515–2535.

Tables

Table 1 Primers used for PCR

Genes	Primers
miR-199a-5p	Forward: 5’-CAATCGCTTTCAAATAG-3’
	Reverse: 5’-CAGGAGATGCTGTCATC-3’
U6	Forward: 5’-CTCGCTTCGGCAGCACA-3’
	Reverse: 5’-AACGCTTCACGAATTTGCGT-3’
HIF-1α	Forward: 5’-TGATTGCATCTCCATCTCCTACC-3’
	Reverse: 5’-GACTCAAAGCGACAGATAACACG-3’
β-actin	Forward: 5’-TTGCGTTACACCCTTTCTTG-3’
	Reverse: 5’-TGCTGTCACCTTCACCGTTC-3’

Figures

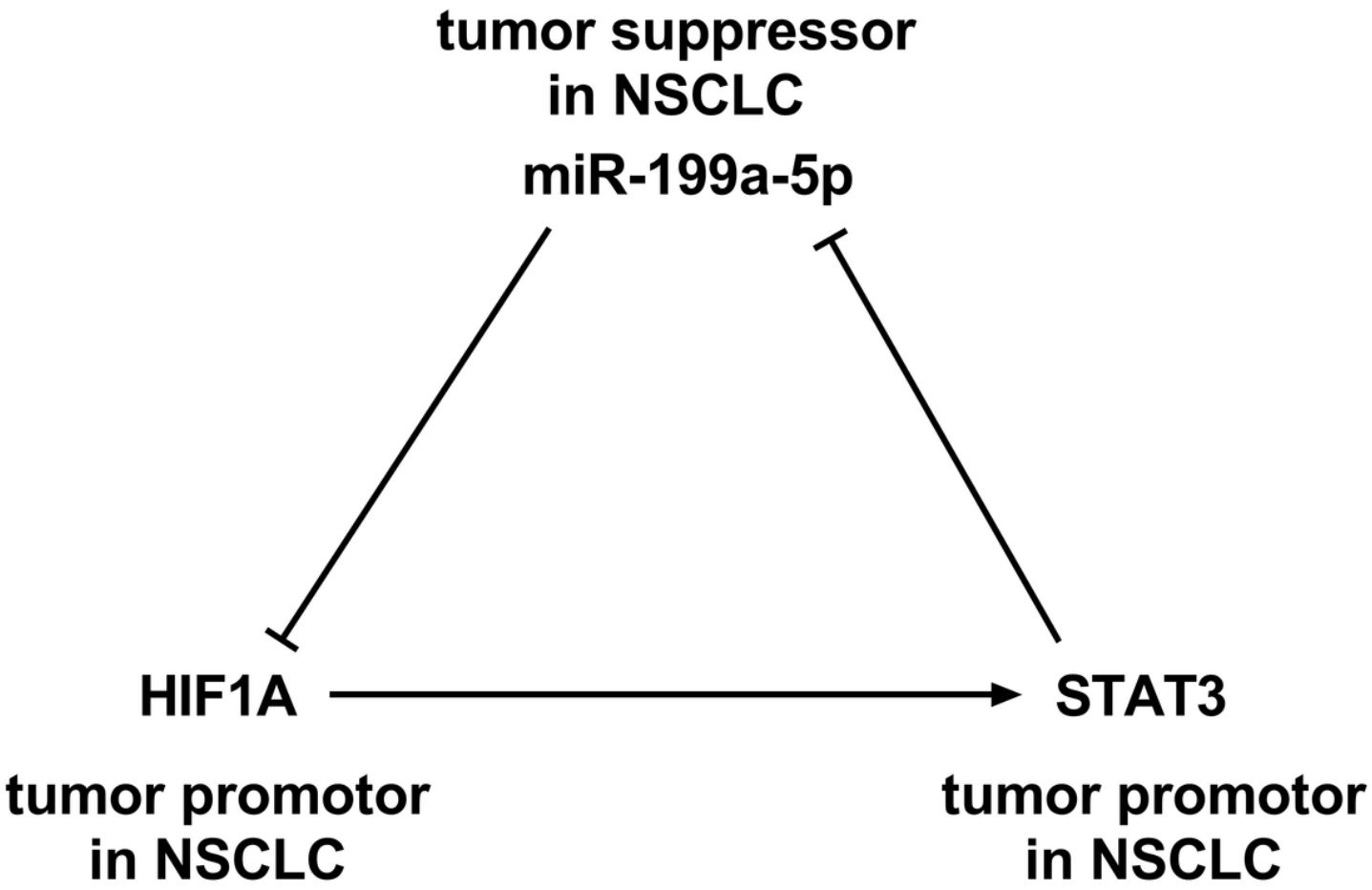

Figure 1

A positive feed-back loop among miR-199a-5p, HIF-1α and STAT3

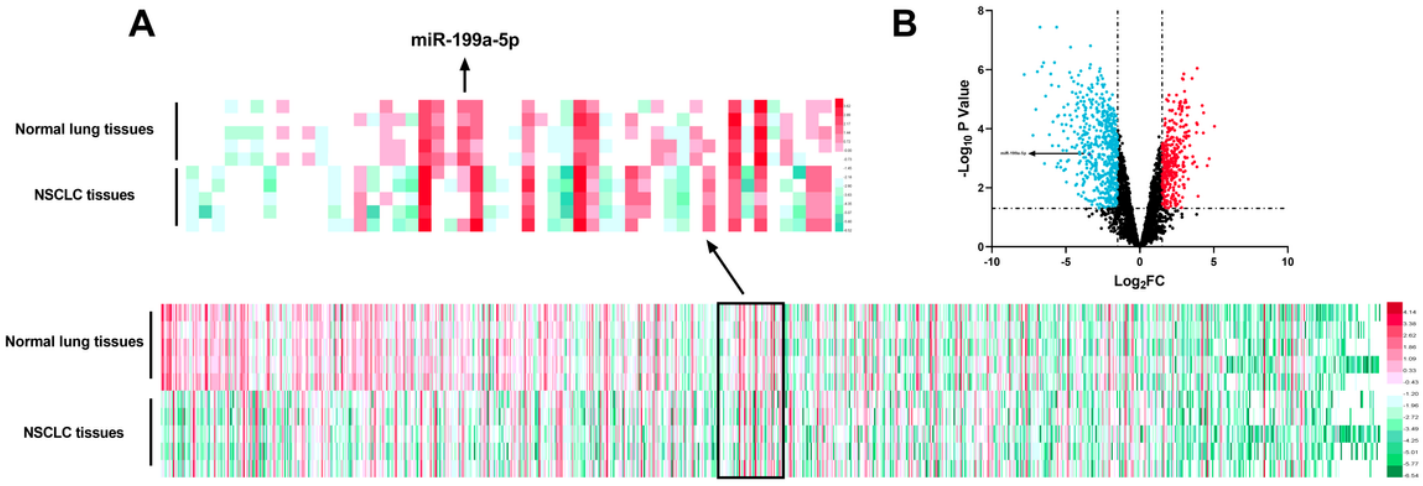

Figure 2

Expression of miRNAs in GSE135981 The heatmap and volcano plot were established with data in GSE135981. (A) MiRNAs with significant changes of expression level between tumor tissues versus normal lung tissues and |log2FC| > 1.5 were shown in heatmap. (B) All the miRNAs were shown in volcano plot and miRNAs significantly upregulated with log2FC > 1.5 were painted red, while miRNAs significantly downregulated with log2FC < -1.5 were painted green.

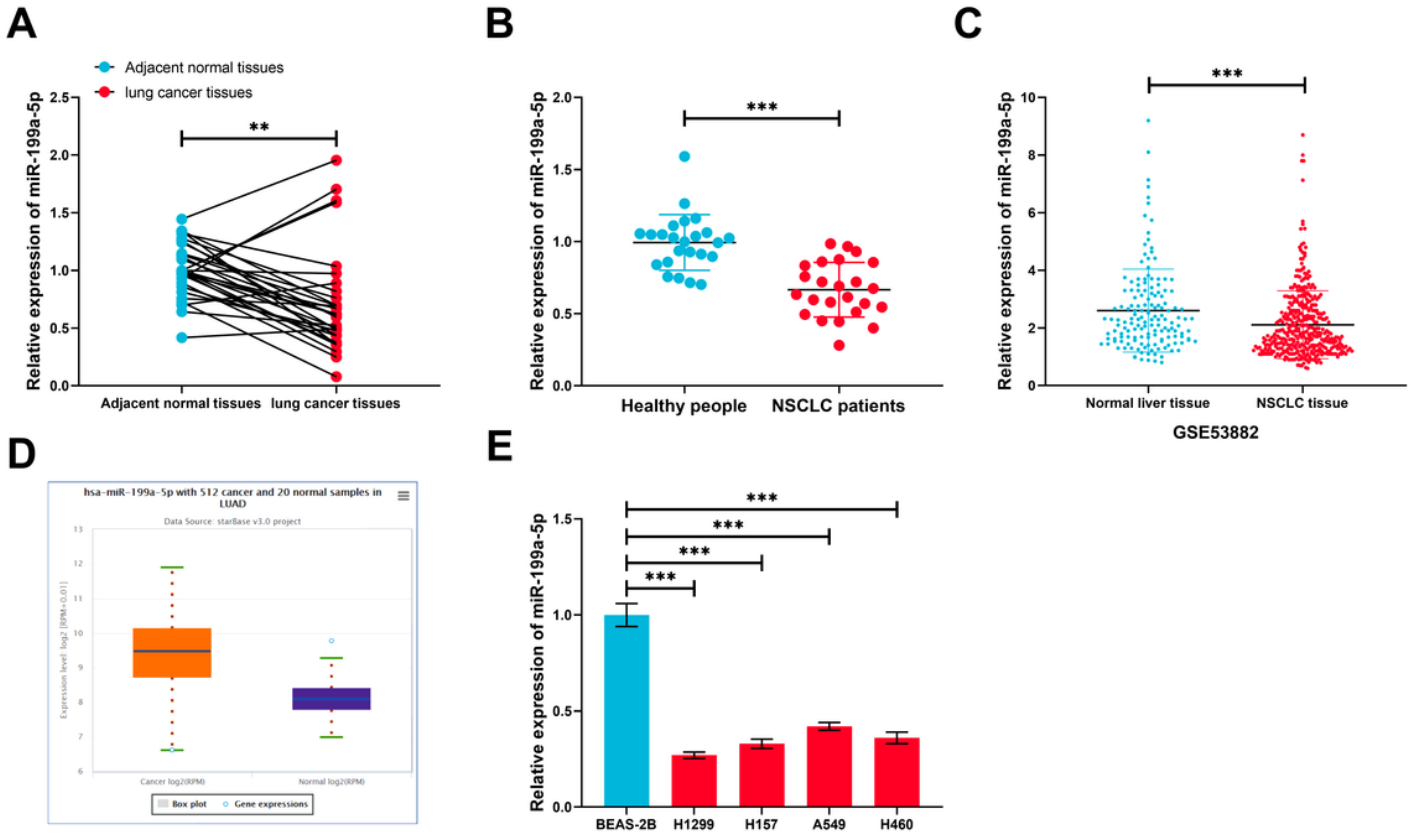

Figure 3

The expression characteristics of miR-199a-5p in NSCLC (A) Expression of miR-199a-5p in NSCLC tissues and adjacent normal lung tissues. (B) Expression of miR-199a-5p in serum samples of NSCLC patients and healthy patients. (C) Expression of miR-199a-5p in 397 NSCLC tissues and 151 normal liver tissues. The data were derived from GSE53882. (D) Expression of miR-199a-5p in lung adenocarcinoma in ENCORI. (E) Expression of miR-199a-5p in normal lung epithelial cells and NSCLC cell lines. **, *** represent $p < 0.01$ and $p < 0.001$, respectively.

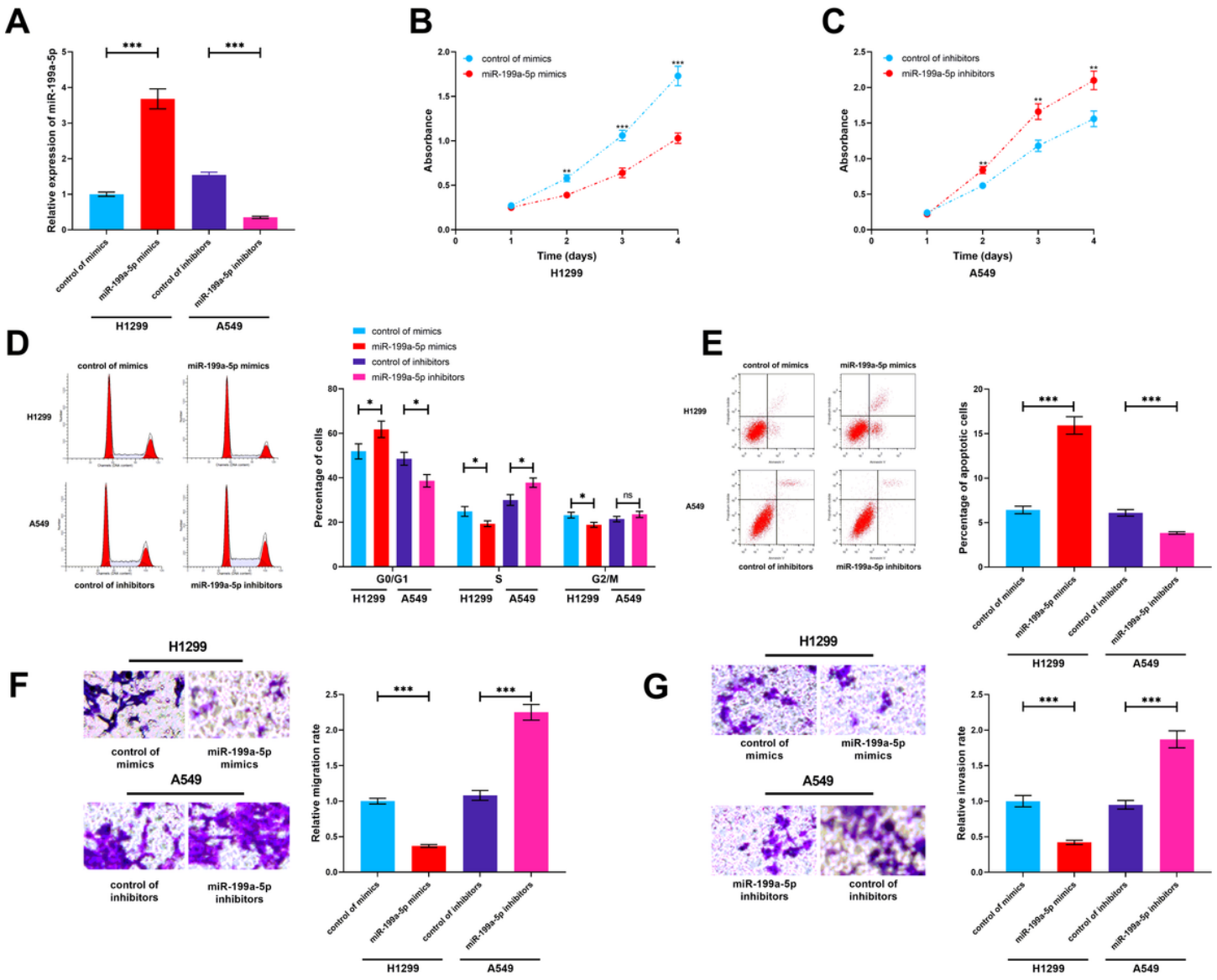

Figure 4

Biological function of miR-199a-5p in NSCLC (A) Transfection efficiency of miR-199a-5p mimics and inhibitors was confirmed by PCR. (B, C) CCK-8 assay was performed to measure proliferation of H1299 and A549 cells. (D, E) Flow cytometry was conducted to analyze cell cycle and apoptosis of H1299 and A549 cells. (F, G) Transwell assay was employed to detect migration and invasion of H1299 and A549 cells. *, ** and *** represent $p < 0.05$, $p < 0.01$ and $p < 0.001$, respectively.

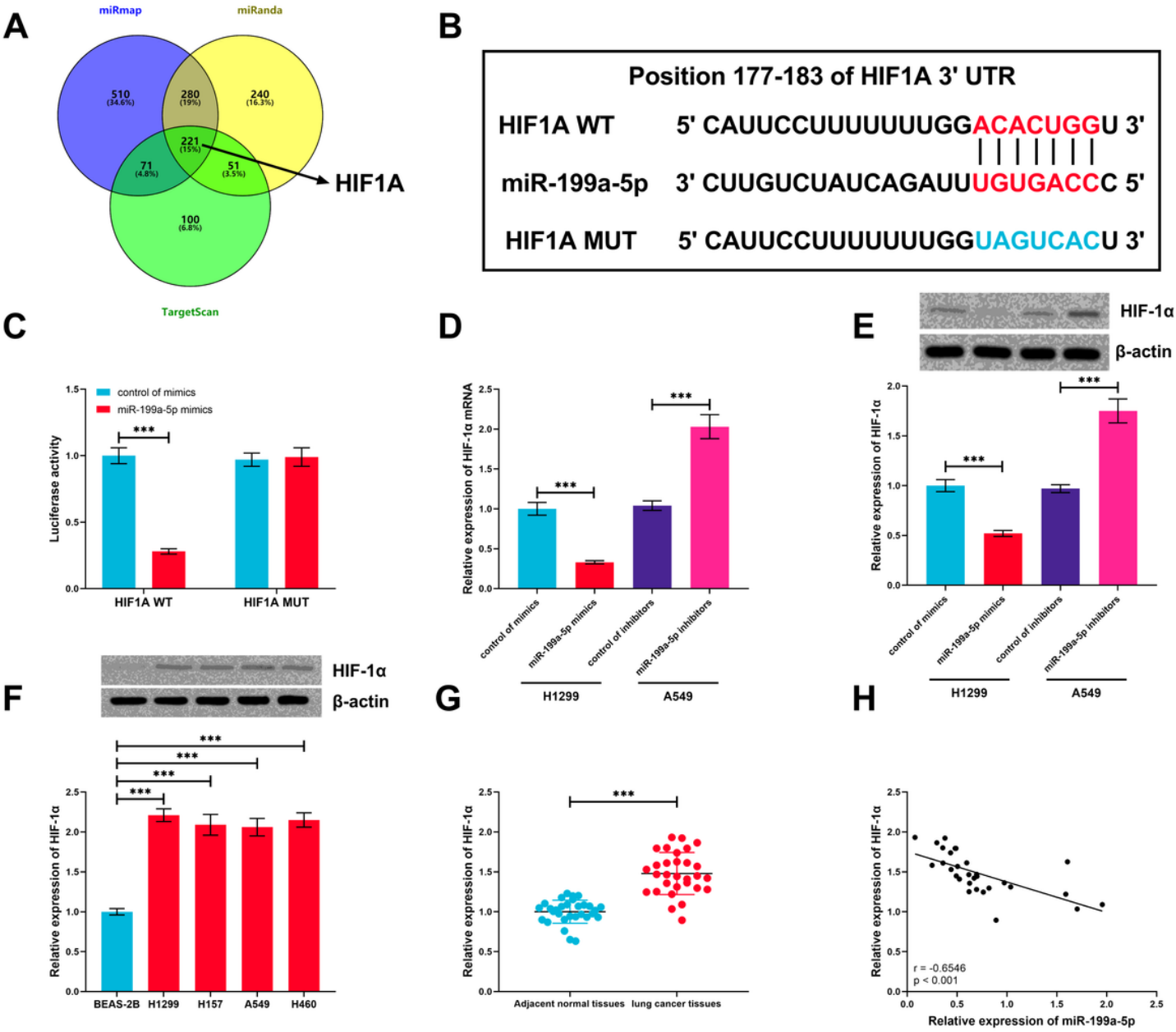

Figure 5

HIF1A was regulated by miR-199a-5p (A) Downstream genes were co-predicted with miRmap, miRanda and TargetScan databases. (B) Conserved binding sequence between HIF1A and miR-199a-5p. (C) Dual-luciferase assay was performed to confirm the binding sites between miR-199a-5p and HIF1A. (D, E) PCR and Western blotting were conducted to measure expression of HIF1A mRNA and HIF1A protein in H1299 and A549 cells. (F) Western blotting was performed to measure HIF-1α protein expression in NSCLC cell lines. (G) Expression of HIF-1α in NSCLC tissues and adjacent normal tissues. (H) Correlation between HIF-1α and miR-199a-5p in NSCLC tissues. *** represents $p < 0.001$.

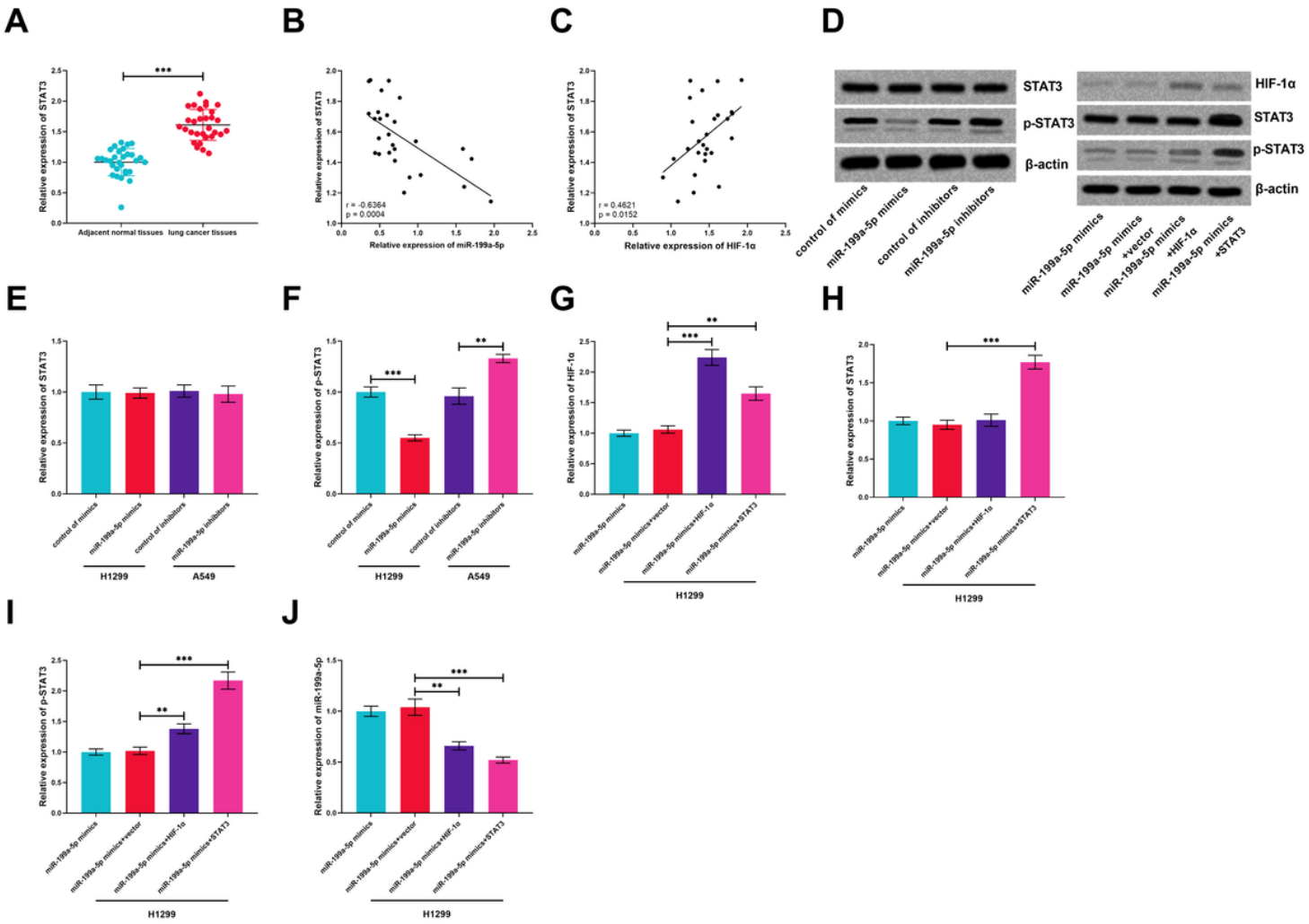

Figure 6

The positive feed-back loop was found between miR-199a-5p, HIF-1α and STAT3 (A) Expression of STAT3 in adjacent normal lung tissues and NSCLC tissues. (B, C) Correlation between STAT3 and miR-199a-5p or HIF-1α in NSCLC tissues. (D) Western blotting for STAT3, p-STAT3 and HIF-1α. (E-J) Relative expression of STAT3, p-STAT3, HIF-1α, and miR-199a-5p after different transfection. ** and *** represent $p < 0.01$ and $p < 0.001$, respectively.

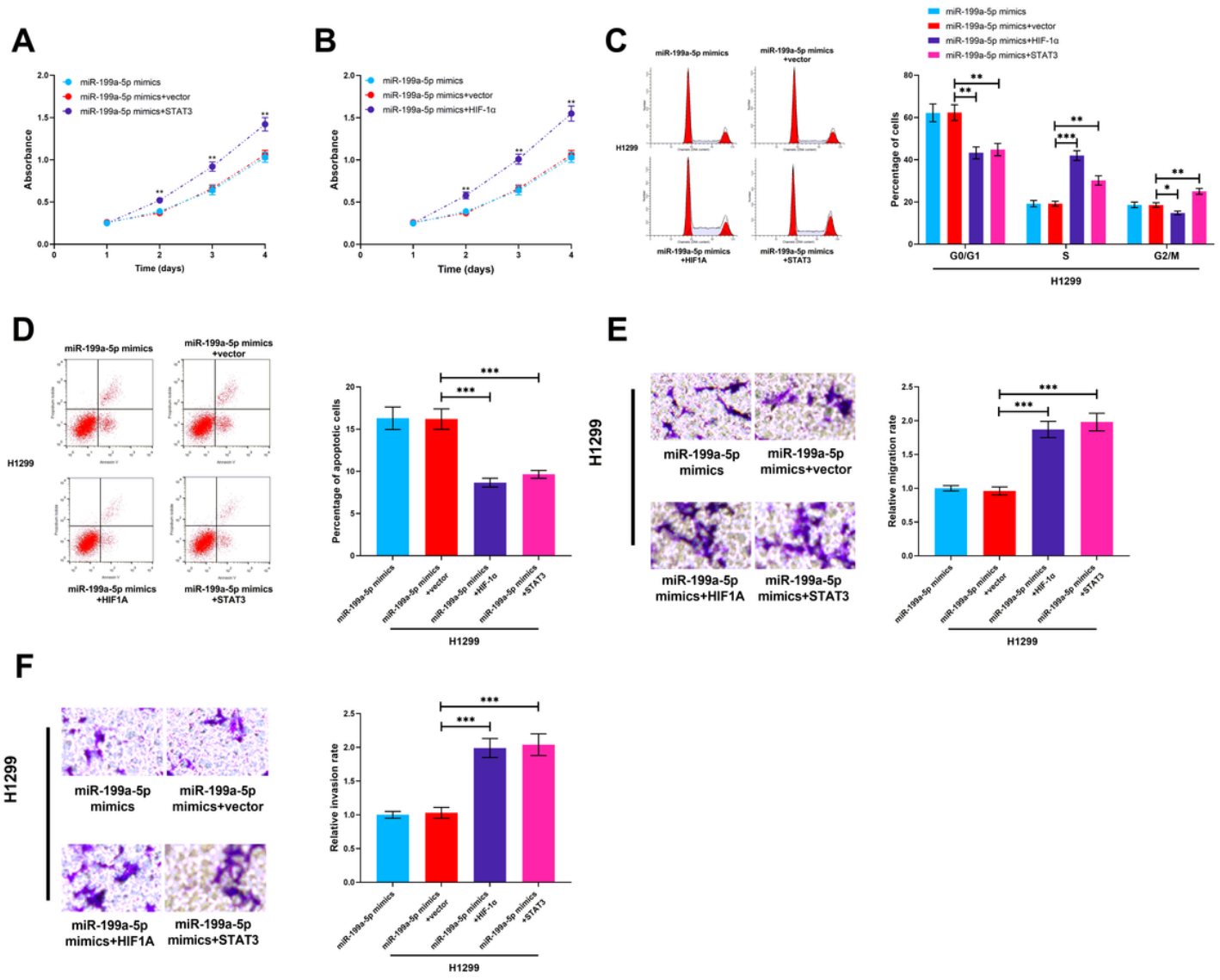

Figure 7

HIF-1α and STAT3 reversed effects of miR-199a-5p (A, B) CCK-8 assay was performed to measure proliferation of H1299 cells. (C, D) Flow cytometry was used to detect H1299 cell cycle and apoptosis. (E, F) Migration and invasion of H1299 cells were analyzed employing Transwell assay. *, ** and *** represent $p < 0.05$, $p < 0.01$ and $p < 0.001$, respectively.

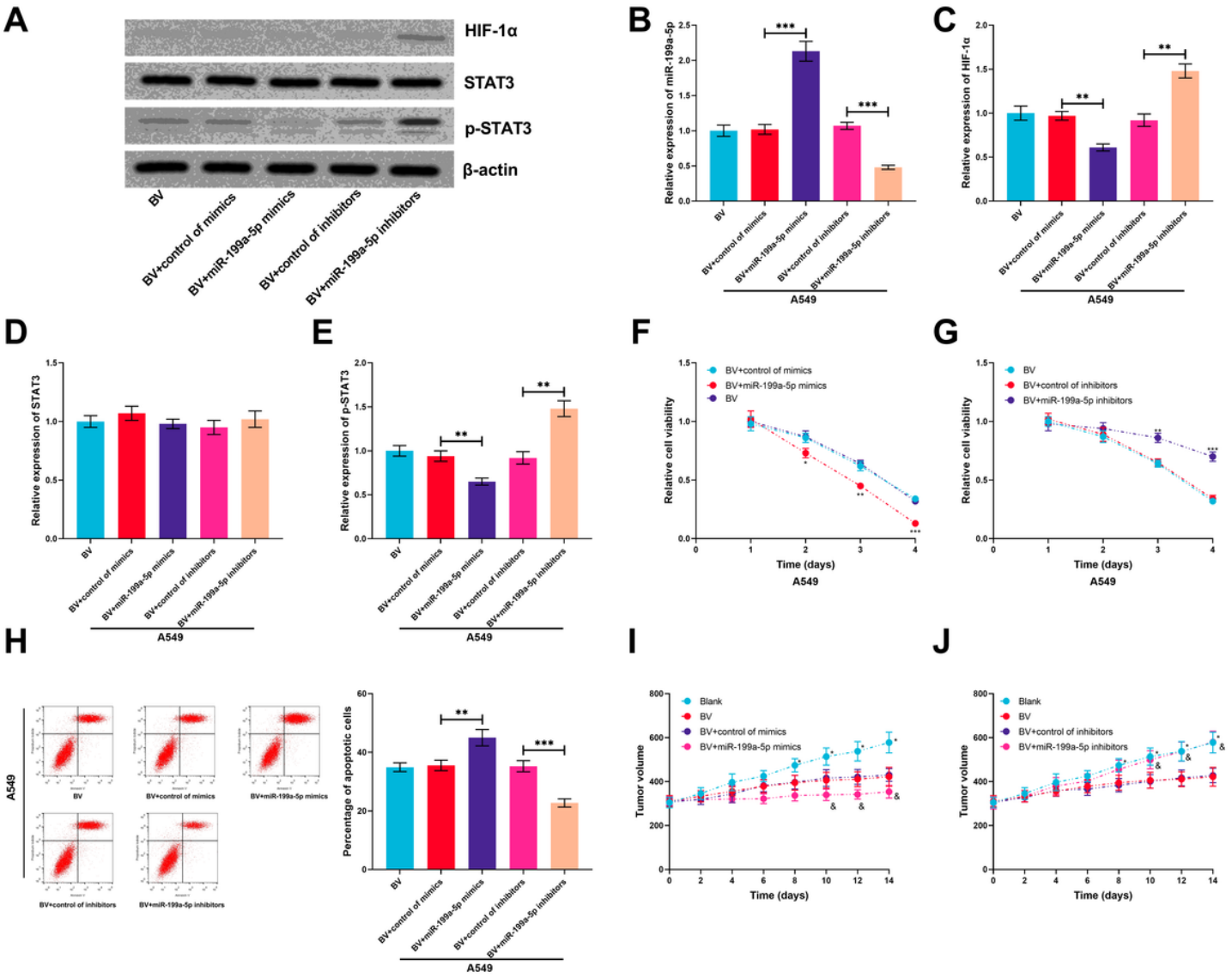

Figure 8

MiR-199a-5p enhanced effects of Bevacizumab on A549 cells (A) Western blotting results of HIF-1α, STAT3 and p-STAT3. (B-E) Relative expression of miR-199a-5p, HIF-1α, STAT3 and p-STAT3. (F, G) Proliferation of A549 cells was validated employing CCK-8 assay. (H) Apoptosis of A549 cells was measured using flow cytometry. (I, J) Changes of A549 tumor volume with time. *, ** and *** represent $p < 0.05$, $p < 0.01$ and $p < 0.001$, respectively. In I and J, & represents $p < 0.05$ BV+control of mimics/inhibitors group versus BV+miR-199a-5p mimics/inhibitors.

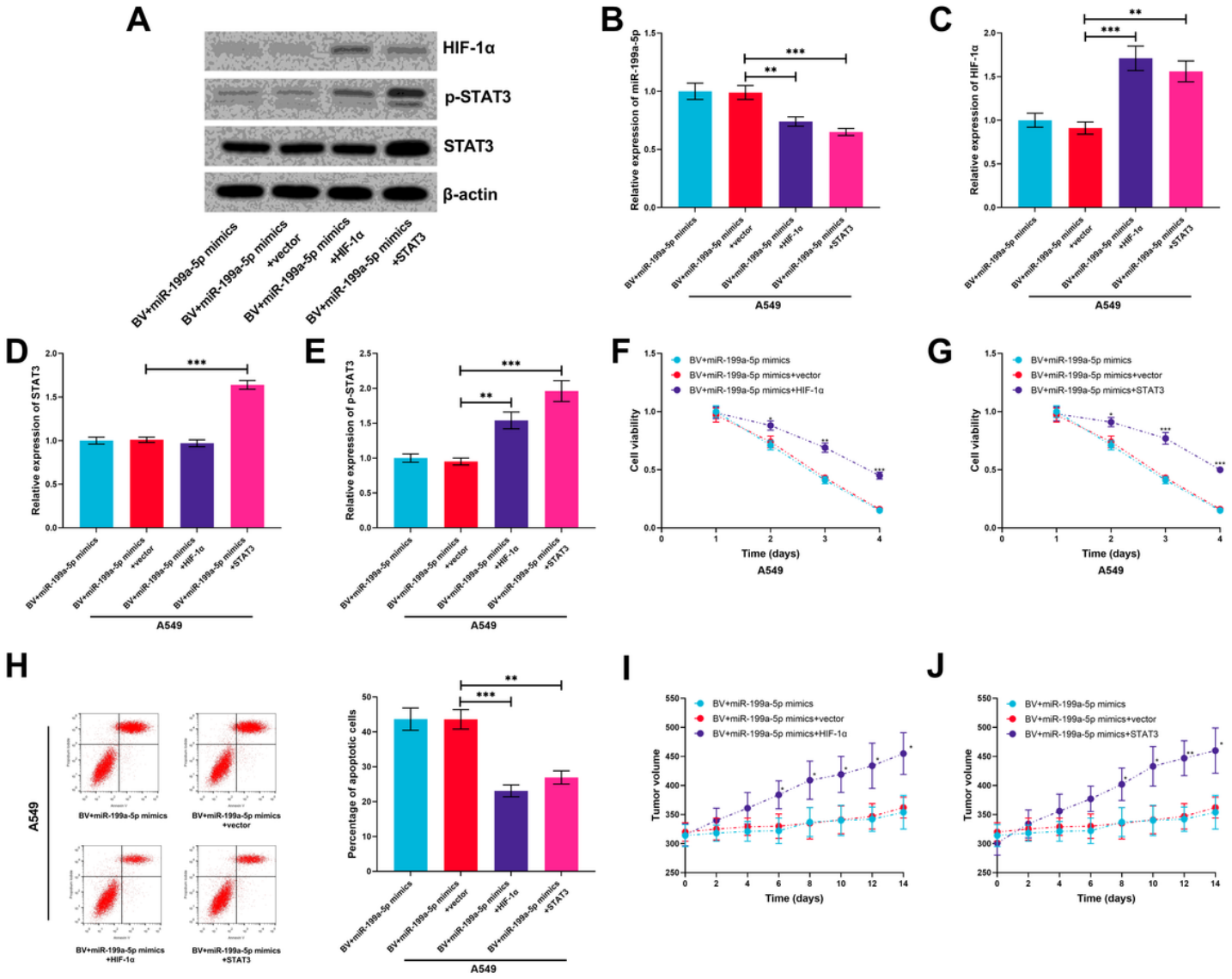

Figure 9

HIF-1α and STAT3 reversed effects of miR-199a-5p on enhancing sensitivity of A549 cells to Bevacizumab (A) Western blotting results of HIF-1α, p-STAT3 and STAT3. (B-E) Relative expression of miR-199a-5p, HIF-1α, STAT3 and p-STAT3. (F, G) Proliferation of A549 cells was measured employing CCK-8 assay. (H) Flow cytometry was employed to analyze apoptosis of A549 cells. (I, J) Changes of A549 tumor volume with time. *, ** and *** represent $p < 0.05$, $p < 0.01$ and $p < 0.001$, respectively.